Cyclohexane Isomerization. Unimolecular Dynamics of the Twist-Boat Intermediate†

Khatuna Kakhiani, Upakarasamy Lourderaj, Wenfang Hu, David Birney, and William L. Hase*

Department of Chemistry and Biochemistry, Texas Tech University, Lubbock, Texas 79409-1061

Received: December 18, 2008; Revised Manuscript Received: January 26, 2009

Direct dynamics simulations were performed at the HF/6-31G level of theory to investigate the intramolecular and unimolecuar dynamics of the twist-boat (TB) intermediate on the cyclohexane potential energy surface (PES). Additional calculations were performed at the MP2/aug-cc-pVDZ level of theory to further characterize the PES's stationary points. The trajectories were initiated at the C_1 and C_2 half-chair transition states (TSs) connecting a chair conformer with a TB intermediate, via an intrinsic reaction coordinate (IRC). Energy was added in accord with a microcanonical ensemble at the average energy for experiments at 263 K. Important nontransition state theory (TST), non-IRC, and non-RRKM dynamics were observed in the simulations. Trajectories initially directed toward the chair conformer had a high probability of recrossing the TS, with approximately 30% forming a TB intermediate instead of accessing the potential energy well for the conformer. The TB intermediate initially formed was not necessarily the one connected to the TS via the IRC. Of the trajectories initiated at the C_2 half-chair TS and initially directed toward the chair conformer, 35% formed a TB intermediate instead of the chair conformer. Also, of the trajectories forming a TB intermediate, only 16% formed the TB intermediate connected with the C_2 TS via the IRC. Up to eight consecutive TB → TB isomerizations were followed, and non-RRKM behavior was observed in their dynamics. A TB can isomerize to two different TBs, one by a clockwise rotation of C−C−C−C dihedral angles and the other by a counterclockwise rotation. In contrast to RRKM theory, which predicts equivalent probabilities for these rotations, the trajectory dynamics show they are not equivalent and depend on whether the C_1 or C_2 half-chair TS is initially excited. Non-RRKM dynamics is also observed in the isomerization of the TB intermediates to the chair conformers. RRKM theory assumes equivalent probabilities for isomerizing to the two chair conformers. In contrast, for the first and following TB intermediate formed, there is a preference to isomerize to the chair conformer connected to the TS at which the trajectories were initiated. For the first TB intermediate formed, approximately 30% of the isomerization is to a chair conformer, but this fraction decreases for the later formed TB intermediates and becomes ∼10% for the eighth consecutive TB intermediate formed.

1. Introduction

Cyclohexane is an archetype molecule for understanding the energetics and isomerization kinetics of conformers.[1] A substantial amount of theoretical and computational effort has been devoted to the conformational analysis of cyclohexane and to establish the fundamental features of its potential energy surface (PES).[2−7] There are two potential energy minima for the lowest energy structure, which is the chair conformation of D_{3d} symmetry. The higher potential energy minima, for which there are six, have a twist-boat structure of D_2 symmetry. Two twist-boat structures are connected via a boat structure transition state (TS) of C_{2v} symmetry. Interconversions between one of the chair structures and each of six twist-boat structures can occur through either of two TSs, one of C_2 symmetry and the other of C_1 symmetry. The geometry of the latter TS has been identified as half-chair.[2,3] The above features of the cyclohexane PES are illustrated in Figure 1.[8] The highest level ab initio electronic structure theory calculations reported for cyclohexane[4] give a 0 K energy difference [zero-point energy (ZPE) included] of 6.7 kcal/mol between the twist-boat and chair potential energy minima, and 0 K barriers of 12.2 kcal/mol for the C_1 and C_2 half-chair TSs connecting the chair and twist-boat minima and of 1.4 kcal/mol for the TS between twist-boat potential energy minima.

The isomerization kinetics between the chair and twist-boat conformers of cyclohexane have been measured in both solution and in the gas-phase.[9−14] For cyclohexane interconversion in solution, $\Delta H^{\ddagger}$ was found to be 10.8 kcal/mol in CS_2 at 173 K[10] and 10.0 ± 0.3 kcal/mol for methyl cyclohexane interconversion in CS_2 at 225 K.[11] This barrier is noticeably less than the $\Delta E^{\ddagger}$ (0 K) ab initio barrier of 12.2 kcal/mol connecting the two chair potential minima.[4] In the gas phase at 263 K,[12,13] the chair−chair interconversion barrier $\Delta H^{\ddagger}$ is 12.1 ± 0.5 kcal/mol, similar to the above ab initio value. In an argon matrix at ∼70 K, the twist-boat to chair $\Delta G^{\ddagger}$ barrier is 5.27 ± 0.05 kcal/mol,[14] and similar to the $\Delta E^{\ddagger}$ (0 K) ab initio barrier of 5.5 kcal/mol.[4]

Theoretical and computational studies have addressed the dynamics of cyclohexane isomerization.[15−23] RISM calculations of the cyclohexane PES in liquid CS_2 indicate that the isomerization free energy barrier increases with increasing density of the solvent,[15] contrary to the experimental finding[11] that the isomerization rate increases with increasing density. From molecular dynamics simulations of cyclohexane isomerization in liquid CS_2, using model analytic potentials,[16] it has been concluded that intramolecular vibrational energy redistribution (IVR)[24] in cyclohexane is inefficient and the isomerization

† Part of the "George C. Schatz Festschrift" Special Issue.

10.1021/jp811208g CCC: $40.75
Published on Web 03/16/2009

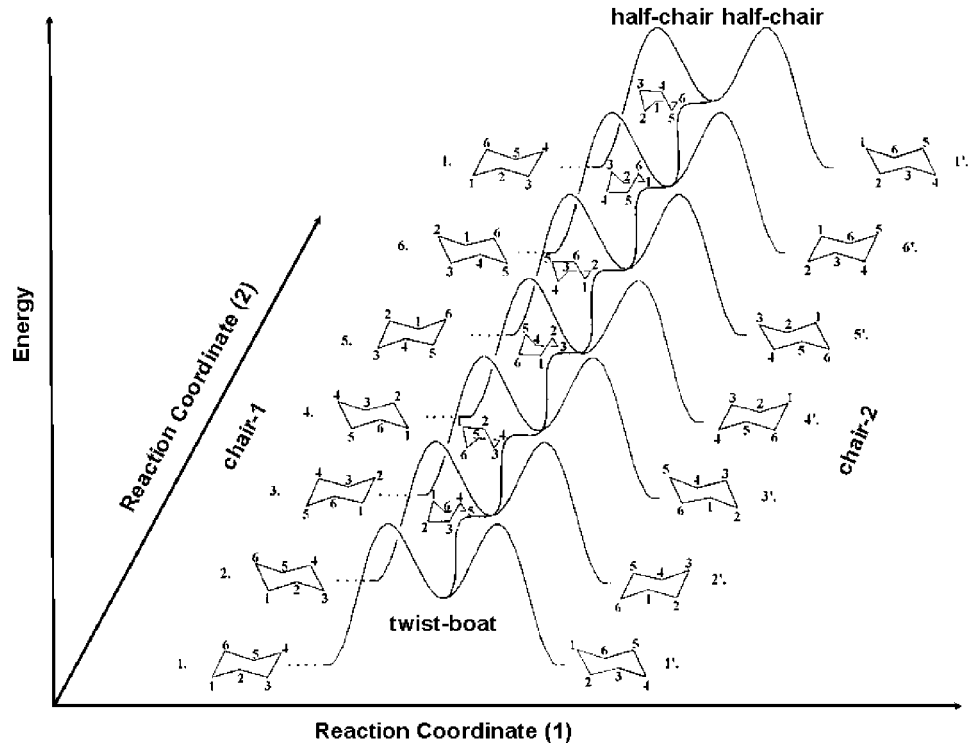

Figure 1. Schematic of the PES for cyclohexane ring inversion. The half-twist TS corresponds to the half-chair TS for the work reported here. (Adapted and used with permission from the *Journal of Chemical Education* **1997**, *74*, 813.)

kinetics not in accord with RRKM theory. Analyses of the trajectories[17] indicate a significant fraction of the intramolecular motion is quasiperiodic[25] for excited cyclohexane. A model,[18] which assumes a "bottleneck" different than that given by the transition state[26−28] controls the isomerization kinetics, has been used to interpret the proposed non-RRKM kinetics. The isomerization rate constant in the gas phase has been determined from a reactive flux simulation[19] based on the reaction path Hamiltonian model and the HF/6-31G PES. Quasiperiodic recrossing of the TS was observed, giving a rate constant different than that of TST but similar to those of condensed phase molecular dynamics simulations[16] and experiments.[10,29] Molecular dynamics simulations, utilizing analytic potential energy functions, have investigated transitions between the different conformers of cyclohexane.[20−23]

Given the archetypical role of cyclohexane in chemistry in general,[8] and organic chemistry in particular,[1,3] it is important to obtain an atomic-level understanding of the possible non-RRKM and non-TST dynamics in its isomerization kinetics. This requires an understanding of both the intramolecular dynamics of the cyclohexane conformers and the unimolecular dynamics for their transitions. Relevant issues include identifying the vibrational modes which may lead to a bottleneck, or bottlenecks, for IVR within a chair conformer, the nature of the weak vibrational coupling leading to possible recrossing of the TSs which connect a chair conformer with a twist-boat conformer, and the nature of the intramolecular and unimolecular dynamics of the six twist-boat conformers.

In the work presented here, direct dynamics trajectories[30−32] at the HF/6-31G level of theory are used to study the dynamics of the twist-boat intermediates. The trajectories are initialized at C_1 and C_2 half-chair TSs connecting chair and twist-boat conformers, with random initial conditions[33] as assumed by TST and RRKM theory. An emphasis is placed on studying the dynamics of trajectories which immediately form the twist-boat intermediate. Of interest are the twist-boat → twist-boat and twist-boat → chair unimolecular dynamics found from the trajectories and their comparisons with the predictions of RRKM theory. Also presented is a comparison of ab initio energies for stationary points on the cyclohexane PES and a comparison of the gas-phase chair → chair rate constants determined from TST, using the ab initio PES, and measured experimentally.[12,13] In future work, an emphasis will be placed on studying the intramolecular and unimolecular dynamics of the chair conformers. With respect to the current study, there is considerable interest in studying the post-transition state dynamics for a chemical reaction after it passes a rate-controlling TS.[34,35]

2. Electronic Structure Calculations

In previous work,[4,6,7,19] stationary points for the cyclohexane PES have been studied using the HF, MP2, and DFT methods and different basis sets. In the work presented here MP2/aug-cc-pVDZ theory, implemented in the NWChem computer program,[36,37] is used to supplement these calculations. Geometries for the stationary points, optimized at the HF/6-31G, MP2/6-31G, B3LYP/6-31G, and MP2-aug-cc-pVDZ levels of theory, are summarized in Table 1. Values are given for the ranges of C−H and C−C bond lengths, and the six torsion angles $\tau_1-\tau_6$; i.e., $C_1C_2C_3C_4$, $C_2C_3C_4C_5$, $C_3C_4C_5C_6$, $C_4C_5C_6C_1$, $C_5C_6C_1C_2$, $C_6C_1C_2C_3$. The torsion angles are defined in the conventional way, in that positive and negative signs correspond to clockwise and counterclockwise rotation about the middle C−C bond, respectively. The four levels of theory give similar geometries. In particular, there are no significant differences between the lowest and highest level, i.e., HF/6-31G and MP2/aug-cc-pVDZ, geometries. There are two chair conformers and six twist-boat (TB) conformers, and a total of 12 TSs of C_2 symmetry and 12 TSs of C_1 symmetry connecting the chair and TB conformers. These TSs are identified as half-chair. Two TB conformers are connected via a boat TS of C_{2v} symmetry. Conformers for each of the five different types of stationary points are illustrated in Figure 2.

TABLE 1: Electronic Structure Stationary Point Geometries[a]

	HF 6-31G	MP2 6-31G	MP2 aug-cc-pVDZ	B3LYP 6-31G
		Chair		
C−H	1.086−1.088	1.102−1.104	1.102−1.105	1.098−1.101
C−C	1.535	1.550	1.535	1.543
τ_1	−54.89	−55.22	−56.28	−54.75
τ_2	54.89	55.22	56.28	54.75
τ_3	−54.89	−55.22	−56.28	−54.75
τ_4	54.89	55.22	56.28	54.75
τ_5	−54.89	−55.22	−56.28	−54.75
τ_6	54.89	55.22	56.28	54.75
		C_2 Chair ↔ TB Half-Chair TS		
C−H	1.084−1.088	1.100−1.104	1.100−1.105	1.097−1.101
C−C	1.528−1.559	1.543−1.576	1.530−1.563	1.539−1.568
τ_1	−13.45	−13.03	−13.38	−13.93
τ_2	−7.29	−7.97	−7.98	−6.88
τ_3	47.97	49.09	49.78	47.67
τ_4	−69.47	−70.99	−72.07	−69.25
τ_5	47.97	49.09	49.78	47.67
τ_6	−7.29	−7.97	−7.97	−6.88
		C_1 Chair ↔ TB Half-Chair TS		
C−H	1.084−1.088	1.100−1.104	1.100−1.105	1.097−1.101
C−C	1.528−1.559	1.543−1.576	1.530−1.563	1.536−1.568
τ_1	−13.29	−13.11	−13.37	−13.93
τ_2	−8.05	−8.312	−9.01	−7.17
τ_3	48.64	49.475	50.81	48.03
τ_4	−69.44	−70.97	−72.04	−69.40
τ_5	47.33	48.626	48.72	47.52
τ_6	−6.75	−7.475	−6.95	−6.66
		TB		
C−H	1.085−1.087	1.101−1.103	1.101−1.104	1.097−1.099
C−C	1.532−1.545	1.548−1.56	1.534−1.547	1.541−1.553
τ_1	−63.70	−65.09	−66.76	−63.61
τ_2	30.67	31.28	32.03	30.63
τ_3	30.67	31.28	32.03	30.63
τ_4	−63.70	−65.09	−66.76	−63.61
τ_5	30.67	31.28	32.03	30.63
τ_6	30.67	31.28	32.03	30.63
		TB ↔ TB Boat TS		
C−H	1.085−1.086	1.101−1.102	1.101−1.102	1.098−1.099
C−C	1.535−1.553	1.551−1.571	1.536−1.559	1.544−1.563
τ_1	−52.43	−53.20	−54.47	−52.74
τ_2	52.42	53.20	54.47	52.74
τ_3	0.00	0.00	0.00	0.00
τ_4	−52.43	−53.20	−54.47	−52.74
τ_5	52.42	53.20	54.47	52.74
τ_6	0.00	0.00	0.00	0.00

[a] The range of C−H and C−C bond lengths are given in angstroms, and the torsion angles τ_1-τ_6 are given in degrees. The torsion angles are given for one of the conformers for each type of stationary point.

Harmonic frequencies were calculated for the stationary points at the HF/6-31G level of theory and used to calculate zero-point energy corrections, temperature corrections to the enthalpies, and RRKM and TST rate constants. These frequencies are listed in Table 2. Frequencies were also calculated with MP2/aug-cc-pVDZ and used to calculate the TST rate constant for this level of theory.

Energies for the stationary points, calculated with different theoretical methods and basis sets, are listed in Table 3. The HF and MP2 energies are quite similar, but those obtained with DFT are lower, particularly the BLYP values. Significant for the HF/6-31G direct dynamics reported here, are the only small differences between the HF/6-31G and much higher level MP2/aug-cc-pVDZ energies. The MP2/aug-cc-pVDZ value for the chair → TB 0 K activation energy with ZPE included, i.e., $\Delta E^{\ddagger}$(0 K), is 12.42 kcal/mol and in overall good agreement with the gas-phase experimental $\Delta H^{\ddagger} = 12.1 \pm 0.5$ kcal/mol at 263 K,[12,13] which if corrected for temperature using the HF/6-31G frequencies gives a 0 K activation energy with the same value, i.e., $\Delta E^{\ddagger}$ (0 K) = 12.1 ± 0.5 kcal/mol. Neglecting the DFT values, the ab initio values for $\Delta E^{\ddagger}$ (0 K) are in the range of 11.83−12.42 kcal/mol. At ∼70 K in an argon matrix, the twist-boat (TB) → chair $\Delta G^{\ddagger}$ barrier is 5.27 ± 0.05 kcal/mol.[14] After correction for temperature and entropy effects, the resulting $\Delta E^{\ddagger}$ (0 K) barrier is 5.43 ± 0.05 kcal/mol. If the DFT values are not included, the ab initio values are in the range of 5.38−6.25 kcal/mol for this barrier, with the HF/6-31G value the lowest and the MP2/aug-cc-pVDZ value the highest. The difference between the gas-phase MP2 value of 6.25 kcal/mol and the experimental condensed-phase value of 5.43 kcal/mol is significant and indicates there may be a condensed-phase effect on the TB → chair barrier and/or the reaction may have important nonstatistical effects. The latter are discussed below along with the direct dynamics results.

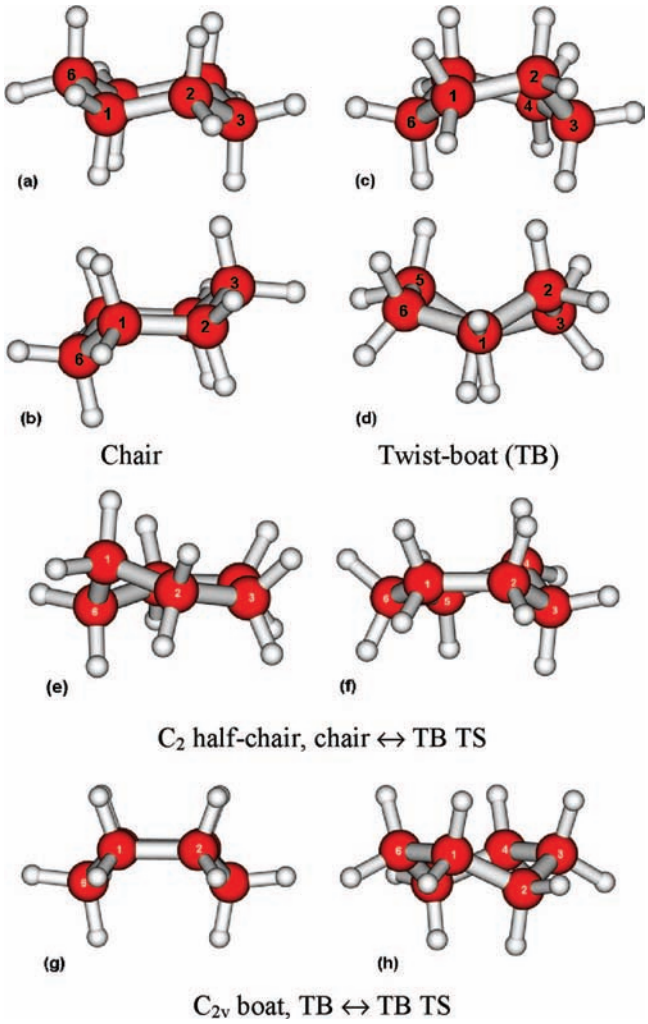

Figure 2. Representative conformers for four types of stationary points on the cyclohexane PES. (a and b) The two chair potential minima; (c and d) two of the six twist-boat (TB) potential minima; (e and f) two of the twelve C_2 half-chair conformers, which are TSs connecting the chair and twist-boat minima; (g and h) two of the six boat conformers, which are TSs connecting two of the twist-boat minima.

3. RRKM and Transition State Theory Calculations

A. RRKM Rate Constants. It is of interest to compare the results of the direct dynamics simulations with the predictions of RRKM unimolecular rate theory.[38] As discussed below, the direct dynamics simulations are initiated, with a microcanonical ensemble of energy, at both a C_1 and C_2 half-chair transition state, connecting chair and twist-boat (TB) conformers. The quantum mechanical vibration and reaction coordinate energy for this ensemble is 1.6 kcal/mol, which is the average thermal internal energy of the TS for the 263 K temperature representative of the experiments.[12,13] For the HF/6-31G PES used in the direct dynamics simulations, the resulting vibrational energy of the TB intermediate, with respect to its ZPE level, is 7.8 kcal/mol. The classical vibrational energy of the TB intermediate, with respect to its classical potential energy minimum and with ZPE included, is 122.5 kcal/mol. The TS's rotational energy is 0.8 kcal/mol, which corresponds to *RT*/2 added to each of its rotation axes, with $T = 263$ K. The average value, of the rotational quantum number J, is 48 for this 263 K rotational excitation.

Harmonic quantum and classical RRKM unimolecular lifetimes,[38] in picoseconds, are listed in Table 4 for the TB → TB, TB → chair, and chair → TB isomerization pathways on the HF/6-31G PES. The RRKM calculations are performed for the above TB energies with J equal to both 0 and 48. Both quantum and classical RRKM calculations are also included for chair → TB isomerization. The RRKM calculations were performed[39] using the equation

$$k(E,J) = \frac{1}{h}\frac{\sum_{K=-J}^{J} N^{\#}[E - E_0 - E_r^{\#}(J,K)]}{\sum_{K=-J}^{J} \rho[E - E_r^{\#}(J,K)]} \qquad (1)$$

which assumes the K rotational quantum number is an active degree of freedom.[40−42] Here, E is the total energy of either the chair or TB conformer, E_o is the barrier for unimolecular decomposition, the E_r are the symmetric top rotational energies for the transition state and conformer, $N^{\ddagger}$ is the transition state's

TABLE 2: Harmonic Frequencies for Stationary Points on the Cyclohexane PES[a]

Chair					
245	245	401	468	468	577
851	878	878	925	925	1018
1018	1129	1129	1148	1187	1188
1255	1313	1416	1416	1416	1416
1506	1516	1518	1518	1537	1537
1648	1648	1650	1650	1660	1668
3165	3165	3167	3167	3168	3169
3212	3212	3216	3216	3219	3229
C_1 Chair → TB[b] Half-Chair TS					
240.8*i*	45	326	474	496	697
806	818	853	926	931	1036
1037	1101	1142	1165	1207	1264
1294	1325	1421	1425	1431	1441
1489	1515	1521	1524	1545	1548
1653	1653	1659	1664	1672	1688
3167	3169	3171	3174	3189	3199
3208	3209	3221	3221	3229	3249
C_2 Chair → TB Half-Chair TS					
240.7*i*	46	326	474	496	697
806	818	853	926	931	1036
1037	1101	1142	1165	1207	1264
1294	1325	1421	1425	1431	1441
1489	1515	1521	1524	1545	1548
1653	1653	1659	1664	1672	1688
3167	3169	3171	3174	3189	3199
3208	3209	3221	3221	3229	3249
Twist-Boat (TB) Intermediate					
116	250	291	467	510	618
843	854	857	923	932	1006
1040	1121	1126	1152	1192	1228
1283	1304	1387	1395	1426	1437
1494	1507	1513	1520	1535	1536
1651	1653	1657	1662	1670	1679
3170	3172	3175	3182	3190	3192
3206	3211	3222	3229	3232	3243
TB → TB Boat TS					
100.5*i*	229	316	483	507	620
846	852	854	921	929	992
1057	1115	1125	1155	1197	1233
1299	1300	1383	1403	1431	1440
1502	1506	1515	1517	1534	1542
1648	1652	1656	1666	1672	1681
3171	3173	3175	3185	3193	3197

[a] HF/6-31G frequencies in cm^{-1}. [b] TB is the twist-boat intermediate.

TABLE 3: Energies for Stationary Points on the Cyclohexane PES[a]

	stationary points		
method	chair ↔ TB[b] half-chair TS	TB intermediate	TB ↔ TB boat TS
HF/6-31G[c]	11.93	6.46	7.41
HF/DZ+P[d]	12.21, 12.25	6.79	7.92
HF/TZ+P[d]	12.35, 12.42	6.95	8.10
MP2/DZ+P[d]	12.42, 12.49	6.95	8.44
MP2/TZ+P[d]	12.30, 12.38	6.82	8.30
MP2/aug-cc-pVDZ[e]	12.52, 12.52	6.18	7.82
B3LYP/6-31G[c]	11.28	6.23	7.06
B3P86/6-311+G**[f]	10.6	6.1	-
BLYP/TZVP(A2)[g]	9.27	5.98	6.68
expt. gas-phase[h]	12.2 ± 0.5	-	-
expt. condensed-phase[i]	10.8		

[a] The energies listed are the classical potential energies (kcal/mol) and are relative to the chair potential energy minimum. They do not include zero-point energies (ZPE). Using the harmonic HF/6-31G vibrational frequencies, the ZPE corrections to the relative energies are −0.10, −0.02, and −0.09 kcal/mol for the chair ↔ TB TS, TB intermediate, and TB ↔ TB TS, respectively. TB represents the twist-boat intermediate. [b] If two energies are given, the first is for the C_2 (TS) and the second for the C_1 (TS); if only one is given, it is for the C_2 (TS). [c] From ref 19. [d] From ref 4. [e] This work. [f] From ref 7. The harmonic HF/6-31G vibrational frequencies were used to calculate the classical barrier from the reported $\Delta H^{\ddagger}$. [g] From ref 6. [h] Determined from the experimental activation enthalpy, $\Delta H^{\ddagger} = 12.1 \pm 0.5$ kcal/mol at 263 K,[12,13] using the HF/6-31G harmonic frequencies. [i] Determined from the experimental activation enthalpy, $\Delta H^{\ddagger} = 10.8$ kcal/mol at 173 K,[10] using the HF/6-31G harmonic frequencies.

sum of states, and ρ is the conformer's density of states. For the classical RRKM calculations the ZPE is included in the total energy. Both classical and quantum RRKM rate constants are included, because it is not evident which is more appropriate for the current study. The classical value should be used if the ZPE flows freely in the simulations. On the other hand, if the vibrational motion retains a degree of adiabaticity with restricted ZPE flow, the quantum RRKM value may be more accurate.

Because classical mechanics place no restrictions on the flow of ZPE, the classical RRKM rate constants exceed their quantum analogues.[43] For the TB → TB isomerization the unimolecular barrier is small, ∼1 kcal/mol, and the classical lifetimes are only ∼1.7 times smaller than the quantum values. However, the TB → chair pathway has a much higher barrier of ∼5.5 kcal/mol and the classical lifetime is orders of magnitude shorter. The difference between the classical and quantum RRKM lifetimes is even greater for chair → TB isomerization, which has a barrier of ∼12 kcal/mol. Of particular interest is the shorter classical RRKM lifetime for the TB → chair pathway as compared to the TB → TB pathway, even though the latter has a much lower potential energy barrier. This is a result of the lower vibrational frequencies for the TB → chair half-chair TS as compared to those for the TB → TB boat TS (see Table 2) and the high total energy of the TB intermediate for the classical RRKM calculation (see footnote d of Table 4). It should be noted that the short lifetimes for TB → TB isomerization are comparable to the periods for the low frequency vibrations of the TB intermediate; e.g., the period for the 116 cm^{-1} vibration is 0.3 ps in comparison to the classical RRKM lifetimes of 0.16−0.25 ps. Finally, the RRKM rate constants were calculated using the harmonic approximation for the sum and density of states. Given the flexibility and low-frequency vibrations for the stationary points on the cyclohexane PES, anharmonic corrections may be important.[38,44−46] An approximate anharmonic correction is considered in Section 4.B.3.

B. Transition State Theory Rate Constant for Chair ↔ Chair Isomerization. The HF/6-31G vibrational frequencies in Table 2 and the MP2/aug-cc-pVDZ frequencies (not listed) for the chair conformer and the chair ↔ TB C_1 and C_2 half-chair TSs, along with a value for the TS's potential energy barrier, were used with transition state theory (TST) to calculate the chair ↔ chair isomerization rate constant and compare with experiment. A chair conformer can access one of the TB intermediates via either one of the six C_1 or six C_2 half-chair TSs. The statistical assumption is that 1/2 of these intermediates return to the reactant chair conformer. The remainder forms the product chair conformer, giving a chair → chair reaction path degeneracy of 3 for both the C_1 and C_2 reaction pathways.

The potential energy barriers for the C_1 and C_2 chair → TB half-chair TSs are the same and, with zero-point energy included, are 11.83 and 12.42 kcal/mol for the HF/6-31G and MP2/aug-cc-pVDZ methods, respectively. TST rate constants for chair → chair isomerization, using the HF/6-31G frequencies, a reaction path degeneracy of 3 for both the C_1 and C_2 reaction pathways, and both the HF/6-31G and MP2/aug-cc-pVDZ potential energy barriers are plotted in Figure 3. The 232−273 temperature range considered is that studied experimentally by Ross and True.[12,13] The HF barriers give TST rate constants that overestimate the experimental values, while the MP2/aug-cc-pVDZ barriers give rate constants in excellent agreement with experiment. Using a barrier of 12.1 kcal/mol for both the C_1 and C_2 TSs, which is close to the MP2/TZ+P values of Dixon and Komornicki,[4] gives TST rate constants larger than the experimental values.

4. Chemical Dynamics Simulations

A. Simulation Methodology. ***1. Trajectory Integration and Initial Conditions.*** The simulations were performed by direct dynamics,[30−32] using the HF/6-31G level of theory. In direct dynamics, the trajectories are integrated "on the fly", with the potential energy, gradient, and also Hessian obtained directly from an electronic structure theory without the need for an analytic potential energy function. The chemical dynamics computer program VENUS,[47] interfaced with the NWChem-4.7 electronic structure theory computer program,[34,35] was used for the simulations. The trajectories were integrated with a Hessian-based predictor−corrector algorithm.[48] A computer processing time of 8 h, on a single dedicated node consisting of Intel Xeon 5345 dual-quad cores (2.33 GHz per core) and 12 GB RAM, was required to integrate a single trajectory for the maximum integration time of 3 ps.

To study the intramolecular and unimolecular dynamics of the twist-boat (TB) intermediates, the trajectories were initiated at both the C_1 and C_2 half-chair TSs which connect the chair-1 conformer with the TB-4 conformer (Figure 4). These TSs are excited with the average vibrational and reaction coordinate translational energy, $\langle E_{vib,rc}^{\ddagger} \rangle$, they have at 263 K, according to TST. This energy is 1.6 kcal/mol and is added randomly so that there is a microcanonical ensemble of states at each TS. For a chemical reaction at a fixed temperature, TST assumes there is a Boltzmann (i.e., canonical) distribution at the TS, with a microcanonical ensemble for each energy in this distribution. A quantum mechanical microcanonical ensemble is sampled[49,50] so that each vibrational level between the zero-point level and 1.6 kcal/mol has equal probability of being populated. The difference between the level's energy and 1.6 kcal/mol is added to reaction coordinate translation. The 1.6 kcal/mol excitation

TABLE 4: RRKM Unimolecular Lifetimes[a,b]

	TB → chair		TB → TB		Chair → TB	
energy[c]	quant.	class.	quant.	class.	quant.	class.
2.40[d]	7.1 (5.4)	0.16 (0.16)	0.37 (0.38)	0.22 (0.22)	164 (105)	0.24 (0.25)

[a] Calculations for the HF/6-31G PES and both harmonic quantum and classical RRKM rate constants are reported. [b] Lifetimes are for $J = 48$, the average value of J for the chair ↔ TB TS at 263 K. Lifetimes in parentheses are for $J = 0$. The reaction path degeneracy for TB → chair is 4, since the TB can isomerize to either chair-1 or chair-2 and there are two half-chair transition states, i.e., C_1 and C_2, for each of these processes. The TB → TB reaction degeneracy is 2, because each TB intermediate can isomerize to two TB intermediates. The chair → TB reaction path degeneracy is 12, because each chair conformer can isomerize to either one of the six TB intermediates, via either a C_1 or C_2 half-chair TS. [c] Energy is in kcal/mol. [d] This is average total energy, i.e., vibration, reaction coordinate translation, and rotation, at the half-chair TS connecting the chair and TB conformers for $T = 263$ K. For the HF/6-31G PES, the resulting quantum total energies of the TB and chair conformers are 7.78 and 14.22 kcal/mol, with respective to their zero-point levels. The resulting classical total energies are 122.45 and 128.92 for the TB and chair conformers.

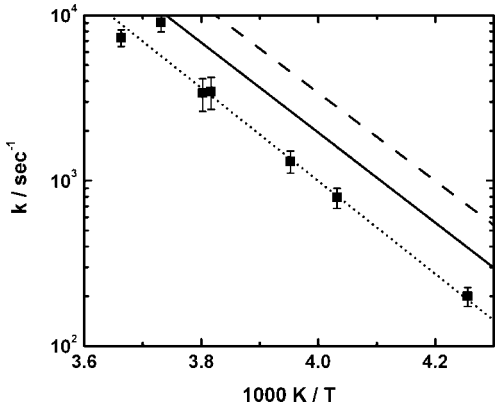

Figure 3. Comparison of TST and experimental[12,13] rate constants (■) for chair → chair isomerization. The TST rate constants were calculated using both the HF/6-31G and MP2/aug-cc-pVDZ for the chair conformer and C_1 and C_2 chair → TB TSs (Table 2), and the potential energies for these TSs. The TST rate constants are: HF/6-31G (---) and MP2/aug-cc-pVDZ (•••). The solid line represents the TST rate constants calculated using the HF/6-31G frequencies and an intermediate barrier of 12.1 kcal/mol for both the C_1 and C_2 pathways.[4]

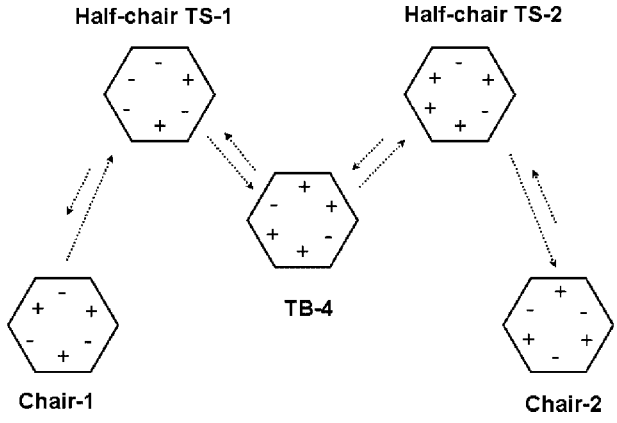

Figure 4. Qualitative depiction of the potential energy curve connecting two chair conformers via a twist boat (TB) intermediate. The trajectories were initiated at the half-chair TS connecting chair-1 and TB-4. Also depicted are the signs of the C−C−C-C torsion angles (see text).

corresponds to 560 cm^{-1}, and only the four lowest frequency vibrational modes of the TS (i.e., 45, 326, 474, and 496 cm^{-1} for the C_1 chair → TB half-chair TS in Table 2) may be excited. The lowest frequency vibrational mode of 45 cm^{-1} may contain up to 12 quanta.

The quasiclassical normal mode sampling method[51,52] was used to prepare a quantum mechanical microcanonical ensemble at the TS. The TS's vibrational energy levels are those for the normal modes, whose vibrational frequencies are given in Table 2. Each level is identified by a set of normal mode quantum numbers n, and a random phase is chosen for each normal mode to transform its energy to its coordinate and momentum. The normal mode eigenvector is then used to transform the normal mode coordinates and momenta to the Cartesian coordinates and momenta used to calculate the trajectories. A energy of $RT/2$, $T = 263$ K, is added to each of the principal rotation axes of the TS by adding the angular velocities, associated with these rotational energies, to the Cartesian momenta for the normal modes. The sign for the reaction coordinate momentum is chosen randomly, so that the trajectories are initially directed randomly toward either the minimum of the chair conformer or that of the TB intermediate.

2. Trajectory Analyses. The classical trajectories were analyzed for short-time recrossing of the barrier for the initially excited half-chair TS connecting the chair-1 and TB-4 conformer (Figure 4), and the unimolecular dynamics of the TB conformer formed by motion from the initially excited half-chair TS and of other TB intermediates formed by ensuing TB → TB isomerizations. Each TB intermediate can isomerize to either of the two chair conformers or to two of the other five TB intermediates (see Figure 1). Of particular interest is the time that excited cyclohexane resides in one of the TB or chair conformers. The average of this time, for the trajectory ensemble, may be compared with the prediction of RRKM theory. Beyer and Schuster, in their MD calculations on the same system,[20] used the sequence of the signs of torsional angles to identify the various conformers of cyclohexane,[3] and we follow their convention in this work. The τ_1 ($C_1C_2C_3C_4$) torsional angle is defined by rotation about the C_2-C_3 bond. When the $C_1C_2C_3$ plane is rotated clockwise toward the $C_2C_3C_4$, τ_1 is considered positive (0 to +180°). A counterclockwise rotation renders τ_1 negative (−180 to 0°). As illustrated in Table 1 and Figure 5, the six torsional angles τ_1, τ_2, τ_3, τ_4, τ_5, and τ_6 which are defined by any four adjacent C atoms in the carbon ring, have the same absolute value of ∼56° (MP2/aug-cc-pVDZ calculations) but alternating signs in a chair conformer.

In moving from a chair conformer to a half-chair TS, connecting a chair and a TB conformer, one of the torsion angles changes sign. This is illustrated in Figure 4 for the chair-1 ↔ TB-4 ↔ chair-2 transitions. As shown in Figure 5, for a boat TS connecting two TB conformers, the six torsion angles are divided into groups of two, each pair sharing their terminal C atoms. One pair is 0°, and the other two are +54.5° and −54.5°, respectively. In the twist-boat conformers, there still exist these three pairs of torsional angles, only that two of them now become equal and are either +32.0° or −32.0°, while another pair takes values of −66.8° or +66.8°. The combination of the signs of the torsional angles is unique for the conformers.

During a TB to TB transition, two torsion angles at opposite ring positions, change sign and pass through zero at the

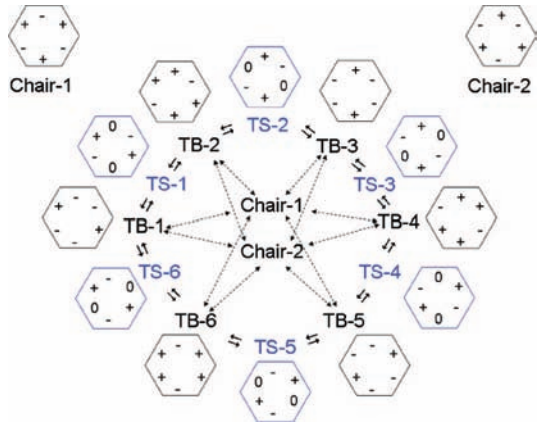

Figure 5. Depiction of the signs of the torsion angles for the chair and twist-boat (TB) conformers and of the transition states connecting these conformers. Each TB intermediate can isomerize to either the chair-1 or chair-2 conformer.

connecting TS. The time cyclohexane spends at this boat TS with two zero torsion angles is infinitesimally small and, thus, the time for the TB → TB transition is well-defined. A half-chair TS, mediating a chair ↔ TB transition, does not have a zero torsion angle, and during a trajectory there is a finite time of finding cyclohexane in the TS's conformation with its torsion angles. However, this time is quite small and from the simulations is found on average to be 36 fs for direct motion (without TS recrossing) from the half-chair TS to the TB intermediate, for the trajectories initiated at the C_1 half-chair TS. For the trajectories initiated at the C_2 half-chair TS, this time is 32 fs. In comparing a trajectory lifetime with the RRKM lifetime, the TS lifetime should be zero. Thus, these times are included in the lifetime of the first TB intermediate formed in the simulations.

The focus of the work reported here is to study the dynamics of the TB conformers and not of the chair conformers. Thus, when a trajectory acquired the torsion angle signs for one of the chair conformers, it was terminated. Because the twist-boat conformers and their boat TSs have approximately the same energy (a difference less than ~1 kcal/mol within the accuracy of our calculations), rapid interconversions among the twist-boat conformers, so-called "pseudorotations", are possible at room temperature and observed in the simulations discussed below.

B. Simulation Results. As discussed above and shown in Figure 4, the trajectories were initiated at both the half-chair C_1 and C_2 TSs for chair-1 → TB-4 isomerization, with random conditions in accord with a microcanonical ensemble at the average energy of isomerizing molecules at 263 K. The sign of the reaction coordinate momentum was chosen randomly so, that for a large trajectory ensemble, 50% of the trajectories would initially move toward either the chair-1 or TB-4 conformer. For the 600 trajectories initiated at the C_1 half-chair TS, 57.0% initially moved toward the TB conformer and the remaining toward the chair-1 conformer. This percentage is 49.7% for the 999 trajectories initiated at the C_2 half-chair TS. Detailed analyses of these trajectories are described in the following.

1. Recrossing Dynamics of the C_1 and C_2 Half-Chair TSs. The fractions of trajectories forming a TB-4 intermediate, for the trajectories initiated at the C_1 and C_2 half-chair transition states (Figure 4), are listed in Table 5. It takes 38 and 34 fs, respectively, for the trajectories initiated at the C_1 and C_2 TSs, and initially directed toward TB-4, to acquire torsion angles

TABLE 5: Recrossing Dynamics of the Initially Excited C_1 and C_2 Half-Chair Transition States[a]

	fraction of trajectories forming the TB intermediate[b]	
TS excited	directed toward TB	directed toward chair[c]
C_1 half-chair	0.80	0.31
C_2 half-chair	0.99	0.35

[a] The trajectories are initiated at the C_1 and C_2 half-chair TS-1 in Figure 4 and randomly directed toward either the chair-1 or TB-4 conformer. [b] The remaining fraction of the trajectories attained the torsion angle for chair-1. [c] The trajectories are stopped when they acquire the torsion angle for chair-1. This is the fraction of trajectories which did not acquire the chair-1 torsion angles and instead returned to the half-chair TS-1 and formed a TB conformer (see text).

for a TB intermediate. For these C_1 trajectories, directed toward TB-4, 0.80 formed a TB intermediate and the remaining recrossed the TS, forming chair-1. For the C_2 trajectories, directed toward TB-4, this fraction is 0.99 and there is negligible recrossing of the TS to form chair-1. Thus, for trajectories directed toward TB-4, the recrossing probability is different for trajectories initiated at the C_1 and C_2 half-chair TSs.

Though the trajectories are directed toward TB-4, when initiated at the C_1 and C_2 half-chair TSs the actual dynamics does not preclude the possibility that the first TB intermediate formed is not TB-4.[53] It is possible that movement off the intrinsic reaction coordinate (IRC) reaction path[54] connecting the TS and TB-4, before TB-4 is formed, may result in the formation of another TB intermediate. This is in fact the type of dynamics that was observed in previous simulations for cyclopropyl radical ring opening,[53] and the $F^- + CH_3OOH$ reaction.[55] Of the trajectories initiated at the C_1 half-chair TS, and directed toward TB-4, 273 formed a TB intermediate and did not recross this TS and form chair-1. Of these 273 TB intermediates formed, 223 were TB-4, 14 TB-3, 34 TB-5, and 2 TB-6. Thus 223/273 = 0.82 of these trajectories formed the TB-4 intermediate toward which they were directed, 36/273 = 0.13 formed a TB intermediate with an index higher than that of TB-4, and 14/273 = 0.05 formed a TB intermediate with a lower index (see Figures 1 and 5 for the relationship between the TB intermediates and their indices). As discussed below, the propensity for motion toward a TB intermediate, with a higher index than that of TB-4, is also seen as for trajectories initiated at the C_1 half-chair TS but initially directed toward chair-1.

For the trajectories initiated at the C_2 half-chair TS and directed toward TB-4, there are equal probabilities for initially forming either TB-3 or TB-5 and, thus, the dynamics is different than that described above for the C_1 half-chair TS. Of the 493 C_2 half-chair TS trajectories directed toward TB-4, 358 form a TB intermediate and the fractions forming TB-4, TB-3, and TB-5 are 358/493 = 0.73, 72/493 = 0.14, and 63/493 = 0.13.

There is substantial TS recrossing for the trajectories initiated at both the C_1 and C_2 half-chair TSs and initially directed toward chair-1. The fraction of these trajectories which formed a TB intermediate, instead of chair-1, is 0.31 and 0.35, respectively, for the trajectories initiated at the C_1 and C_2 half-chair TSs. It took 58 fs for these C_1 TS initiated trajectories to acquire the torsion angles for a TB intermediate and 49 fs for these C_2 TS initiated trajectories. As for the trajectories initially directed toward TB-4, the first TB intermediate formed was not necessarily TB-4. Of the 79 trajectories initiated at the C_1 half-chair TS and directed toward chair-1, but which recrossed the TS before acquiring the torsion angles for chair-1, 1, 12, 44, 19,

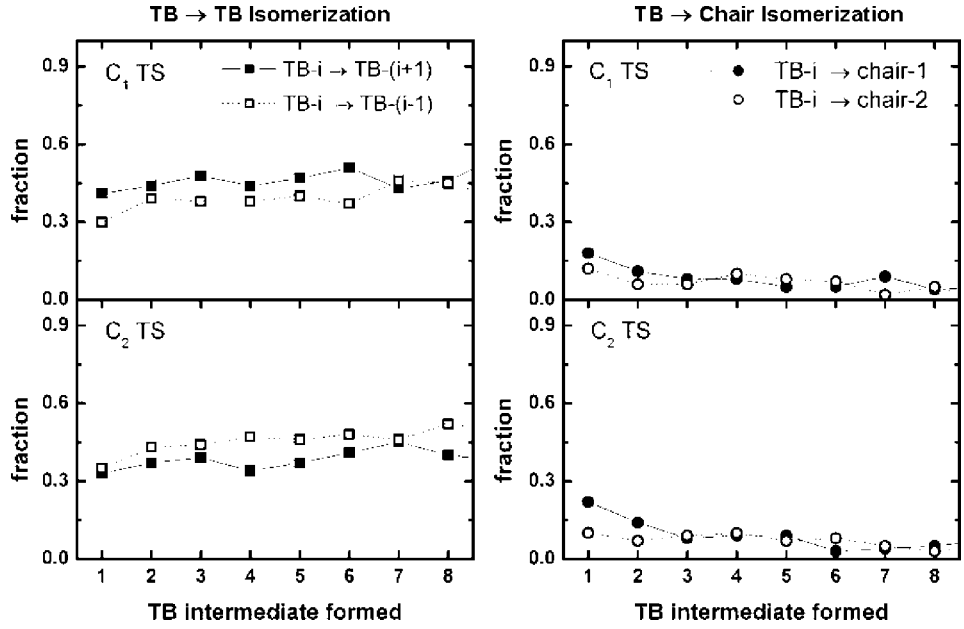

Figure 6. Left side: for each of the consecutive TB intermediates formed, plotted are the fractions of the intermediate's trajectories isomerizing to a TB intermediate with a higher index (i+1), ■, and a lower index (i−1), □. Right side: for each of the consecutive TB intermediates formed, plotted are the fractions of the intermediate's trajectories isomerizing to chair-1, ●, and chair-2, ○.

and 3 initially formed TB-2, TB-3, TB-4, TB-5, and TB-6, respectively. Thus, there is the same propensity, as found above, for initially forming a TB intermediate with an index higher than that of TB-4, instead of lower.

Considerably different dynamics were found for the trajectories initiated at the C_2 half-chair TS and directed toward chair-1. Here, 178 trajectories formed a TB intermediate instead of chair-1, and the numbers of trajectories forming the different TB intermediates are 2, 70, 28, 73, and 5 for TB-2, TB-3, TB-4, TB-5, and TB-6, respectively. Thus, the most likely TB intermediate to be formed is not TB-4, but a neighboring intermediate TB-3 or TB-5.

The times required for trajectories initially directed toward TB-4 and chair-1, to first acquire the torsion angles for a TB intermediate are 38 and 58 fs for the trajectories initiated at the C_1 half-chair TS, and 34 and 49 fs for the trajectories initiated at the C_2 half-chair TS. From these times, and taking into account the weights of the respective trajectories, one can estimate the time it takes an average trajectory to first acquire torsion angles for a TB intermediate as it moves directly (without TS recrossing) from the half-chair TS toward the TB intermediates. This time is 36 fs for the trajectories initiated at the C_1 half-chair TS and 32 fs for the trajectories initiated at the C_2 half-chair TS. These times are included in the lifetimes of the first TB intermediates formed.

It should be recognized that the above fractions of trajectories which recross the half-chair TS, after their initial direction toward chair-1, may be an underestimate of such short-time TS recrossing. This is because the trajectories are terminated as soon as the torsion angle signs acquire the values for chair-1. It is certainly possible that all of these terminated trajectories do not have a long lifetime in the chair-1 region of the phase space, as predicted by RRKM theory, and instead an appreciable fraction may recross the half-chair TS in short times.

2. Unimolecular Branching Ratios for the TB Intermediates. The TB-i intermediate formed by the trajectories, initiated at the half-chair TS, can isomerize to chair-1 or chair-2 or to TB-(i−1) or TB-(i+1). The probabilities of these four unimolecular reactions for TB-4, and such reactions for ensuing TB intermediates that are formed, are plotted in Figure 6. Results are given for the consecutive TB intermediates formed in the simulations.

Each of the consecutive intermediates can undergo an isomerization to a TB intermediate with a higher or lower i-index. For the first TB intermediate, these isomerizations are TB-i → TB-(i+1) and TB-i → TB-(i−1). For the next isomerizations, there are two pathways to a higher i-index, i.e. TB-(i−1) → TB-(i) and TB-(i+1) → TB-(i+2), and two pathways to a lower i-index, i.e. TB-(i−1) → TB-(i−2) and TB-(i+1) → TB-(i). Of interest is a possible difference in the probabilities for isomerizing to TB intermediates with higher and lower i-indices. The graphs on the left side of Figure 6 show that there is a tendency for the TB intermediates, resulting from the trajectories initiated at the C_1 half-chair TS, to preferentially isomerize to the TB intermediate with the higher index. If all the TB intermediates are considered, i.e., first to eighth, it is 1.22 times more likely to isomerize to the higher index TB intermediate as compared to the one with the lower index. For the trajectories initiated at the C_2 half-chair TS, the opposite is observed, and it is 1.16 times more likely to form the TB intermediate with the lower index. RRKM theory assumes equivalent probabilities for the isomerizations to the higher and lower indexed TB intermediates.

As shown by the graphs on the right side of Figure 6, a difference with RRKM theory is also observed for the TB → chair isomerizations. Each TB intermediate can isomerize to either chair-1 or chair-2, and RRKM theory predicts equal probabilities for these isomerizations. However, the simulations show that for the first TB intermediate formed, the fraction isomerizing to chair-1 is approximately a factor of 2 higher than to chair-2. The trajectories were initiated at the transition state connecting chair-1 and TB-4 and show a nonstatistical preference for the initially formed TB intermediate to return to chair-1. This preference for isomerizing to chair-1 instead of chair-2 remains for the next TB intermediate formed but not for any of the further consecutive TB intermediates formed. In considering all the TB intermediates, the overall preference to form chair-1 instead of chair-2 is 1.23:1.00 and 1.39:1.00 for the trajectories

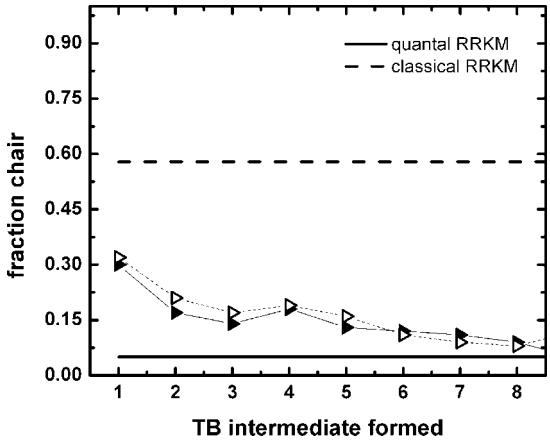

Figure 7. Fraction of the trajectories isomerizing to a chair conformer for each of the consecutively formed TB intermediates. Results are give for the trajectories initiated at both the C_1 (triangle right solid) and C_2 (triangle right open) half-chair TSs. The harmonic RRKM prediction, both classical and quantal, is also given.

initiated at the C_1 and C_2 half-chair TSs, respectively. This short-time non-RRKM dynamics is consistent with apparent non-RRKM behavior,[28] arising from the nonrandom excitation of the initially formed TB intermediate.

The fraction of trajectories which isomerize from a TB intermediate to form a chair conformer instead of another TB intermediate is shown in Figure 7, for each of the consecutive TB intermediates formed during the simulations. This fraction is largest for the first intermediate, because of its preference to form chair-1 and then decreases for the remaining intermediates. The fraction to form a chair conformer, from the initially formed TB intermediate, is 0.30 and 0.32 for the trajectories initiated at the C_1 and C_2 half-chair TSs, respectively. For the latter TB intermediates, and at longer times, this fraction appears to approach a value near 0.10 or slightly lower. Also shown in Figure 7 are the classical and quantal harmonic RRKM predictions for the fraction of trajectories which isomerize from a TB intermediate to form a chair conformer. The quantal fraction is 0.05 and in much better agreement with the long time simulation value of ~0.10 than is the classical fraction of 0.58. There are obvious non-RRKM dynamics in this fraction because it depends on time. In addition, it is not clear why the quantal fraction is in better agreement with the long time simulation value for the fraction than is the classical fraction.

3. Comparison of Trajectory and RRKM Lifetimes. The average lifetimes, obtained from the trajectories, of the first to eighth consecutively formed TB intermediates are 198 ± 9, 160 ± 16, 109 ± 7, 127 ± 17, 124 ± 10, 113 ± 12, 92 ± 6, and 99 ± 8 fs for the trajectories initiated at the C_1 half-chair TS, and 198 ± 8, 123 ± 8, 115 ± 9, 152 ± 11, 150 ± 12, 158 ± 17, 125 ± 12, and 110 ± 11 fs for the trajectories initiated at the C_2 half-chair TS. In comparison, the classical and quantal harmonic RRKM lifetimes are 93 and 352 fs, respectively. The trajectory lifetimes are intermediate of these values. The quantal RRKM lifetime is longer, because of zero-point energy constraints, which require a fixed ZPE for both the TB potential energy minimum and TSs for isomerization of the TB conformer to a another TB conformer or a chair conformer. These constraints are not present for the classical RRKM calculation, and the ZPE is assumed to flow freely among the vibrational degrees of freedom.[41] That the trajectory lifetimes are intermediate between the classical and quantal RRKM values suggests that ZPE is not constrained as assumed by quantal RRKM theory but does not flow freely as assumed by classical RRKM theory. The overall tendency for the trajectory lifetimes to shorten in moving from the first to eighth TB intermediate suggests that the intramolecular dynamics is becoming more classical, without any constraints on ZPE flow, as there is more time for energy flow between the vibrational modes. It should be noted that this analysis is based on harmonic RRKM calculations, and the role of anharmonicity is to decrease the unimolecular rate constants and increase the lifetimes. If the ZPE is assumed to have randomized for the last, i.e. eighth, TB intermediate formed, the trajectory lifetime for this intermediate is the classical anharmonic RRKM lifetime. Combining the lifetimes for the eighth TB intermediate, obtained from the trajectories initiated at the C_1 and C_2 half-chair TSs, gives a lifetime of 106 ± 7 fs for the TB intermediate, suggesting an approximate classical RRKM anharmonic correction factor of (106 ± 7)/93 = 1.14 ± 0.08.

5. Summary

In the work presented here, a direct dynamics simulation at the HF/6-31G level of theory was used to investigate the atomistic dynamics of trajectories initiated at the C_1 and C_2 half-chair TSs separating a chair conformer from a twist-boat (TB) conformer on the cyclohexane PES. Initial conditions were chosen for the trajectories which correspond to a microcanonical ensemble at the average energy of 263 K experiments. The following important non-TST, non-IRC, and non-RRKM dynamics were observed in the simulations.

1. The trajectories initially directed toward the chair conformer had a large probability of recrossing the TS at which they were excited before accessing the chair potential energy minimum. For the trajectories initiated at the C_1 and C_2 half-chair TSs, 31 and 35% of these trajectories recrossed the TS, respectively, and formed a TB conformer instead of the chair conformer toward which they were initially directed. TS recrossings are much less important for the trajectories initially directed toward the TB intermediate. For trajectories initiated at the C_1 half-chair TS, 20% recrossed this TS to form the chair conformer, while there was only 1% recrossing for the trajectories initiated at the C_2 half-chair TS.

2. The C_1 and C_2 half-chair TSs, at which the trajectories were initiated, are connected to a specific TB intermediate via an intrinsic reaction coordinate (IRC) reaction path.[54] However, this is not necessarily the first TB intermediate formed. For the trajectories initiated at the C_1 half-chair TS, and directed toward the IRC TB intermediate, this was the first TB intermediate formed for 82% of the trajectories. For the remaining trajectories, there was nearly a factor of 3 higher probability of forming a TB intermediate with a higher index than that for the IRC TB, as compared to forming a TB with a lower index (see Figure 5). Similar dynamics were found for the trajectories initiated at the C_1 half-chair TS and directed toward a chair conformer but which instead formed TB intermediates. For 56% of the trajectories, the first TB intermediate formed was that for the IRC. Of the remaining trajectories, it was nearly a factor of 2 more probable to form a TB intermediate with a higher index than that for the IRC TB, instead of forming a TB with a lower index.

Considerably different dynamics for forming the TB intermediate were found for the trajectories initiated at the C_2 half-chair TS. Of the trajectories initially directed toward the IRC TB and which formed a TB intermediate, 73% formed the IRC TB with nearly equal probabilities for the remainder to form TB intermediates with an index either higher or lower than that for the IRC TB. For the trajectories initially directed toward

the chair conformer, but which instead formed a TB intermediate, the most probable TB formed is not that for the IRC. The probability of forming the IRC TB is only 16%, and there are nearly equal probabilities for forming a TB intermediate with an index either higher or lower than that for the IRC TB.

3. The TB intermediates exhibit non-RRKM dynamics. Apparent non-RRKM behavior is expected, as a result of the initial nonrandom excitation resulting from the motion from the half-chair TS to the initially formed TB intermediate.[28] Different initial nonrandom excitations of this TB are expected for the trajectories initiated at the C_1 and C_2 half-chair TSs, because they have different structures and, thus, eigenvectors for their normal modes including the reaction coordinate.

RRKM theory assumes that each consecutively formed TB intermediate has equivalent probabilities of isomerizing to a TB intermediate with either a higher or lower index. As shown in Figure 6, this is not observed and the non-RRKM behavior appears to be present for all the consecutively formed TB intermediates and not just the first one formed by the motion from the half-chair TS. For all the TB intermediates formed, first to eighth, it is 1.22 times more probable to isomerize to a TB intermediate with a higher index for the trajectories initiated at the C_1 half-chair TS and 1.16 more probable to isomerize to a TB intermediate with a lower index for the trajectories initiated at the C_2 half-chair TS. The longevity of these dynamics suggest they may arise from intrinsic non-RRKM behavior.[28]

Non-RRKM dynamics is also observed for isomerization of the TB intermediates to the chair conformers. RRKM theory assumes equivalent probabilities for isomerizing to the two chair conformers. In contrast, for the first and next TB intermediate formed there is a preference to isomerize to the chair conformer connected to the half-chair TS at which the trajectories were initiated. That this dynamics only exists for short times indicates it is apparent non-RRKM behavior.[28] Non-RRKM dynamics is also seen in the branching between TB isomerization to a chair conformer versus TB isomerization to another TB conformer. For the first TB conformer formed, approximately 30% of the isomerization is to a chair conformer, but this fraction decreases for the later TB intermediates that are formed and becomes $\sim$10% for the eighth consecutive TB intermediate formed. The simulations indicate that this percentage has not reached a constant value and is still decreasing, and the long time behavior of these non-RRKM dynamics suggests they are intrinsically non-RRKM.[28]

The work presented here suggests several future investigations. The extensive recrossing of the half-chair TS, connecting chair and TB conformers, for trajectories initially directed toward the chair strongly suggests weak couplings within the chair phase space, because the large density of states of the chair's modes does not provide a bath to temporarily trap all the trajectories. Intrinsic non-RRKM dynamics are suggested for isomerization of a chair conformer to a TB conformer. Thus, if a chair conformer is excited randomly, in accord with a microcanonical ensemble, its chair $\rightarrow$ TB isomerization probability will be nonexponential and its gas-phase isomerization rate constant will depend on the total pressure.[56,57] For some pressure regimes, the rate constant may appear to be independent of pressure. It will be of interest to determine whether the chair $\rightarrow$ TB isomerization probability is nonexponential and, if it is, whether it is a biexponential or a more complicated as seen for other non-RRKM dynamics.[56,57]

It will also be important to investigate the cyclohexane potential energy surface at higher levels of electronic structure theory and to perform more accurate TST calculations of the chair-1 $\rightarrow$ chair-2 unimolecular rate constant. As discussed in Section 3.B the MP2/aug-cc-pVDZ potential energy surface, when combined with TST and RRKM theory, gives a chair-1 $\rightarrow$ chair-2 rate constant in excellent agreement with experiment.[12,13] In comparison, important non-RRKM and non-TST effects are observed in the direct dynamics reported here. The TST calculation is highly sensitive to the potential energy of the half-chair TS connecting the chair and TB conformers; e.g., a 0.5 kcal/mol shift in the potential energy of this TS, by a more accurate ab initio calculation, would change the rate constant by a factor of 3 at 263 K. The current TST calculation was performed using harmonic vibrational frequencies, for the chair conformer and half-chair TS, to determine their zero-point energies and vibrational frequencies. For a more accurate TST calculation, anharmonic frequencies would be used to calculate these terms.

Another interesting dynamical question concerns whether the TB intermediates are thermalized at the system temperature for reactions performed in solution. If the energy relaxation between the excited TB intermediates and the solution molecules is slower than the lifetime of a TB intermediate, the TB intermediate will retain a memory of the nonthermal excitation it acquired during its formation. Thermalization may become more important for the TB intermediates formed by consecutive TB $\rightarrow$ TB isomerizations. These thermalization dynamics may be studied by performing the type of direct dynamics reported here in the midst of a bath of solute molecules.[58]

Acknowledgment. This material is based upon work supported by the National Science Foundation under Grant No. CHE-0615321 and the Robert A. Welch Foundation under Grant No. D-0005. The High-Performance Computing Center (HPCC) at Texas Tech University, under the direction of Dr. Philip W. Smith, provided important computational resources and system administration support for the calculations reported here.

Note Added in Proof. Additional electronic structure calculations, with a tighter convergence criterion, were performed for the C1 and C2 half-chair TSs connecting the chair and TB conformers. Though these two TS structures, each with a single imaginary frequency, were identified previously[4] and in the work presented here, these additional calculations indicate that for some (and maybe all) levels of theory these two TS structures may coalesce to a single TS. However, these additional calculations are only suggestive, and more extensive work needs to be performed to prove that this is indeed the case. What both the calculations reported here and these additional ones show is that the chair $\leftrightarrow$ TB TS region is broad and flat, illustrated by the nearly isoenergetic C1 and C2 half-chair TSs. The quasiclassical TS sampling method used here is expected to be accurate if the TS structure is well-localized, with harmonic motion, so that the quadratic Hamiltonian for the saddlepoint has a reaction coordinate eigenvector which describes the motion across the TS and has normal modes which gives the TS vibrational energy.[33,50] However, for a broad, flat TS region this sampling method may be less accurate, since the vibrational motion may be highly anharmonic and the TS crossing motion not localized and, thus, may not be generally defined by a single reaction coordinate eigenvector. Somewhat fortuitously, by sampling both the C1 and C2 TSs with their individual reaction coordinate eigenvectors, as is done here, more representative chair $\leftrightarrow$ TB TS crossing motions may have been obtained. In addition, including two TSs in the TST calculation may in some manner account for TS anharmonicity. Further methodological development is clearly needed to quantitatively sample TS

anharmonic vibrational energy levels quasiclassically,[59] with delocalized TS crossing.

References and Notes

(1) Lowry, T. H.; Schueller-Richardson, K., *Mechanism and Theory in Organic Chemistry*; Harper & Row: New York, 1987.
(2) Hendrickson, J. B. *J. Am. Chem. Soc.* **1961**, *83*, 4537.
(3) Burkert, A.; Allinger, N. L., *Molecular Mechanics*; American Chemical Society: Washington, DC, 1982.
(4) Dixon, D. A.; Komornicki, A. *J. Phys. Chem.* **1990**, *94*, 5630.
(5) Kolossváry, I.; Guida, W. C. *J. Am. Chem. Soc.* **1993**, *115*, 2107.
(6) Smith, B. J. *J. Phys. Chem. A* **1998**, *102*, 3756.
(7) Ionescu, A. R.; Berces, A.; Zgierski, M. Z.; Whitfield, D. M.; Nukada, T. *J. Phys. Chem. A* **2005**, *109*, 8096.
(8) Leventis, N.; Hanna, S. B.; Sotiriou-Leventis, C. *J. Chem. Educ.* **1997**, *74*, 813.
(9) Johnson, W. S.; Bauer, V. J.; Margrave, J. L.; Frisch, M. A.; Dreger, L. H.; Hubbard, W. N. *J. Am. Chem. Soc.* **1961**, *83*, 606.
(10) Anet, F. A. L.; Bourn, A. J. R. *J. Am. Chem. Soc.* **1967**, *89*, 760.
(11) Hasha, D. L.; Eguchi, T.; Jonas, J. *J. Chem. Phys.* **1981**, *75*, 1571.
(a) Hasha, D. L.; Eguchi, T.; Jonas, J. *J. Am. Chem. Soc.* **1982**, *104*, 2290.
(12) Ross, B. D.; True, N. S. *J. Am. Chem. Soc.* **1983**, *105*, 1382.
(13) Ross, B. D.; True, N. S. *J. Am. Chem. Soc.* **1983**, *105*, 4871.
(14) Squillacote, M.; Sheridan, R. S.; Chapman, O. L.; Anet, F. A. L. *J. Am. Chem. Soc.* **1975**, *97*, 3244.
(15) Singer, S. J.; Kuharski, R. A.; Chandler, D. *J. Phys. Chem.* **1986**, *90*, 6015.
(16) Kuharski, R. A.; Chandler, D.; Montgomery, J. A.; Rabii, F.; Singer, S. J. *J. Phys. Chem.* **1988**, *92*, 3261.
(17) Wilson, M. A.; Chandler, D. *Chem. Phys.* **1990**, *149*, 11.
(18) Leitner, D. M. *Adv. Chem. Phys.* **2005**, *130*, 205.
(19) Peters, B.; Bell, A. T.; Chakraborty, A. *J. Chem. Phys.* **2004**, *121*, 4453.
(20) Beyer, A.; Schuster, P. *Monatshefte fur Chemie* **1990**, *121*, 339.
(21) Harris, J. G.; Stillinger, F. H. *J. Chem. Phys.* **1991**, *95*, 5953.
(22) Kawai, T.; Tomioka, N.; Ichinose, T.; Takeda, M.; Itai, A. *Chem. Pharm. Bull.* **1994**, *42*, 1315.
(23) Christensen, I. T.; Jorgensen, F. S. *J. Comp-Aided Molec. Des.* **1997**, *11*, 385.
(24) Hase, W. L. *J. Phys. Chem.* **1986**, *90*, 365.
(25) Wolf, R. J.; Hase, W. L. *J. Chem. Phys.* **1980**, *73*, 3779.
(26) Rice, O. K., Z. Phys. Chem. B 1930, *7*, 226. (quoted by Kassel L. S. *Kinetics of Homogeneous Reactions*; Chemical Catalog: New York, 1932.)
(27) Bunker, D. L. *J. Chem. Phys.* **1964**, *40*, 1946.
(28) Bunker, D. L.; Hase, W. L. *J. Chem. Phys.* **1973**, *59*, 4621.
(29) Allerhand, A.; Chen, F.; Gutowsky, H. S. *J. Chem. Phys.* **1965**, *42*, 3040.
(30) Bolton, K.; Hase, W. L.; Peslherbe, G. H., In Multidimensional Molecular Dynamics Methods; Thompson, D. L., Ed.;World Scientific: London, 1998; pp143−189.
(31) Sun, L.; Hase, W. L. *Rev. Comp. Chem.* **2003**, *19*, 79.
(32) Hase, W. L.; Song, K.; Gordon, M. S. *Computing in Science & Engineering* **2003**, *5*, 36.
(33) Peslherbe, G. H.; Wang, H.; Hase, W. L. *Adv. Chem. Phys.* **1999**, *105*, 171.
(34) Vayner, G.; Addepalli, S. V.; Song, K.; Hase, W. L. *J. Chem. Phys.* **2006**, *125*, 014317.
(35) Lourderaj, U.; Park, K.; Hase, W. L. *Int. Rev. Phys. Chem.* **2008**, *27*, 361.
(36) Kendall, R. A.; Apra, E.; Bernholdt, D. E.; Bylaska, E. J.; Dupuis, M.; Fann, G. I.; Harrison, R. J.; Ju, J.; Nichols, J. A.; Nieplocha, J.; Straatsma, T. P.; Windus, T. L.; Wong, A. T. *Comput. Phys. Commun.* **2000**, *128*, 260.
(37) Bylaska, E. J.; de Jong, W. A.; Govind, N.; Kowalski, K.; Straatsma, T. P.; Valiev, M.; Wang, D.; Apra, E.; Windus, T. L.; Hammond, J.; Nichols, P.; Hirata, S.; Hackler, M. T.; Zhao, Y.; Fan, P.-D.; Harrison, R. J.; Dupuis, M.; Smith, D. M. A.; Nieplocha, J.; Tipparaju, V.; Krishnan, M.; Wu, Q.; Van Voorhis, T.; Auer, A. A.; Nooijen, M.; Brown, E.; Cisneros, G.; Fann, G. I.; Fruchtl, H.; Garza, J.; Hirao, K.; Kendall, R.; Nichols, J. A.; Tsemekhman, K.; Wolinski, K.; Anchell, J.; Bernholdt, D.; Borowski, P.; Clark, T.; Clerc, D.; Dachsel, H.; Deegan, M.; Dyall, K.; Elwood, D.; Glendening, E.; Gutowski, M.; Hess, A.; Jaffe, J.; Johnson, B.; Ju, J.; Kobayashi, R.; Kutteh, R.; Lin, Z.; Littlefield, R.; Long, X.; Meng, B.; Nakajima, T.; Niu, S.; Pollack, L.; Rosing, M.; Sandrone, G.; Stave, M.; Taylor, H.; Thomas, G.; van Lenthe, J.; Wong, A.; Zhang, Z., "NW Chem, A Computational Chemistry Package for Parallel Computers, Version 5.1" (2007), Pacific Northwest National Laboratory, Richland, Washington 99352−0999, USA.
(38) Baer, T.; Hase, W. L., *Unimolecular Reaction Dynamics. Theory and Experiments*; Oxford: New York, 1996.
(39) Zhu, L.; Hase, W. L. Quantum Chemistry Program Exchange (QCPE) Bulletin 14 644(1994).
(40) Zhu, L.; Hase, W. L. *Chem. Phys. Lett.* **1990**, *175*, 117.
(41) Aubanel, E. E.; Wardlaw, D. M.; Zhu, L.; Hase, W. L. *Int. Rev. Phys. Chem.* **1991**, *10*, 249.
(42) Zhu, L.; Chen, W.; Hase, W. L.; Kaiser, E. W. *J. Phys. Chem.* **1993**, *97*, 311.
(43) Hase, W. L.; Buckowski, D G. J. *Comput. Chem* **1982**, 335.
(44) Bhuiyan, L. B.; Hase, W. L. *J. Chem. Phys.* **1983**, *78*, 5052.
(45) Song, K.; Hase, W. L. *J. Chem. Phys.* **1999**, *110*, 6198.
(46) Vayner, G.; Addepalli, S. V.; Song, K.; Hase, W. L. *J. Chem. Phys.* **2006**, *125*, 014317.
(47) Hase, W. L.; Duchovic, R. J.; Hu, X.; Komornicki, A.; Lim, K. F.; Lu, D.-H.; Peslherbe, G. H.; Swamy, K. N.; Vande Linde, S. R.; Zhu, L.; Varandas, A.; Wang, H.; Wolf, R. J. *Quantum Chemistry Program Exchange (QCPE) Bulletin* **1996**, *16*, 671.
(48) Lourderaj, U.; Song, K.; Windus, T. L.; Zhuang, Y.; Hase, W. L. *J. Chem. Phys.* **2007**, *126*, 044105.
(49) Doubleday, C.; Bolton, K.; Peslherbe, G. H.; Hase, W. L. *J. Am. Chem. Soc.* **1996**, *118*, 9922.
(50) Sun, L.; Hase, W. L. *J. Chem. Phys.* **2004**, *121*, 8831.
(51) Sloane, C. S.; Hase, W. L. *J. Chem. Phys.* **1977**, *66*, 1523.
(52) Hase, W. L.; Ludlow, D. M.; Wolf, R. J.; Schlick, T. *J. Phys. Chem.* **1981**, *85*, 958.
(53) Mann, D. J.; Hase, W. L. *J. Am. Chem. Soc.* **2002**, *124*, 3208.
(54) Fukui, K. *J. Phys. Chem.* **1970**, *74*, 4161.
(55) López, J. G.; Vayner, G.; Lourderaj, U.; Addepalli, S. V.; Kato, S.; de Jong, W. A.; Windus, T. L.; Hase, W. L. *J. Am. Chem. Soc.* **2007**, *129*, 9976.
(56) Hase, W. L.; Duchovic, R. J.; Swamy, K. N.; Wolf, R. J. *J. Chem. Phys.* **1984**, *80*, 714.
(57) Peslherbe, G. H.; Wang, H.; Hase, W. L. *J. Chem. Phys.* **1995**, *102*, 5626.
(58) Bolton, K.; Hase, W. L.; Doubleday, C. *J. Phys. Chem. B* **1999**, *103*, 3691.
(59) Song, K.; Peslherbe, G. H.; Hase, W. L.; Dobbyn, A. J.; Stumpf, M.; Schinke, R. *J. Chem. Phys.* **1995**, *103*, 8891.

JP811208G